

Effects of Growth Conditions on Structural and Optical Properties of Porous GaAs Layers

Z. Harrabi^{1*}, L. Beji¹, N. Chehata¹, A. Ltaief¹, H. Mejri² and A. Bouazizi^{1,*}

¹*Equipe Dispositifs Electroniques Organiques et Photovoltaïque Moléculaire, Faculté des Sciences de Monastir, Avenue de l'Environnement, 5019 Monastir, Tunisia.*

²*Unité de Mathématiques Appliquées et de Physique Mathématique, Ecole Préparatoire aux Académies Militaires à Sousse, Rue Maréchal Tito 4029 Tunisia.*

Email: zina_harrabi2000@yahoo.fr

Received: 22 Jul. 2013; Revised: 13 Nov. 2013; Accepted: 29 Nov. 2013; Published: 1 Jul. 2014

Abstract: Porous GaAs was prepared using electrochemical anodization technique of a crystalline GaAs wafer in hydrofluoric (HF) acid based-solution at different manufacturing conditions. The physical properties of porous GaAs are mainly determined by the shape, diameter of pores, porosity, and the thickness of deposited porous layers. Depending on the etching parameters such as current density, HF concentration or substrate doping type and level, the physical properties of porous GaAs can be varied. In the present work, we investigate the structural and optical properties of porous GaAs etched at different current densities. The PL spectra of the porous layers reveal the presence of infrared and visible peaks observed at 1.42 and 1.80 eV respectively. The infrared PL peak is associated with the band gap edge of bulk GaAs and the visible PL band is due to quantum confined transitions in GaAs crystallites, induced by electrochemical etching. Both peak wavelengths and intensities of PL peaks vary as versus the treatment of samples. The refractive index and the extinction coefficient of the as-prepared GaAs have been determined in the 400-1000 nm wavelength range using spectroscopic ellipsometry. These optical parameters are in agreement with the Bruggeman effective medium model. As has been found, the refractive index at 632 nm increases from 1.42 to 1.74 with increasing the film thickness from 52 to 154 nm and decreasing the porosity from 78 to 68 per cent.

Keywords: Porous GaAs, Electrochemical anodization, Photoluminescence (PL), X-ray diffraction.

1. INTRODUCTION

The discovery of intense visible photoluminescence [1, 2, 3] in porous Si formed by electrochemical etching has led to an increased interest in porous semiconductors. Opposite to porous Si, few works have been carried out on III-V semiconductors [4]. Pore formation has reported so far in InP [5, 6], GaP [7,8] and GaAs [9-11]. The porous III-V semiconductors have gained considerable importance because of their attractive optoelectronic properties due to the quantum confinement effects. Mostly, GaAs is considered of large interest because the elaborated porous GaAs layers using anodization technique present a luminescence behavior in the visible region and at higher energies than porous silicon [12,13]. Porous GaAs is often electrochemically formed in solutions containing HF [14] or HCl [15]. The promising luminescence properties of porous GaAs opens up a variety of applications in GaAs-based integrated optoelectronics devices such as light emitting diodes.

Furthermore, few reports focused on the growth of porous structure of p- GaAs substrate [16]. A promising approach is to obtain various porous semiconducting materials using electrochemical etching. This method has a number of advantages: (i) it is fairly simple and inexpensive, (ii) in the case of a positive result, it would become possible to extend the spectral range of luminescence response and thus to fabricate new types of light-emitting diodes. By varying etching parameters such as current density, etching time, electrolyte composition [1], the physical properties of porous GaAs can be also varied. In this work, porous GaAs has been prepared under different current densities. The porous GaAs layers were characterized by an atomic force microscopy (AFM), X-ray diffraction, photoluminescence and spectroscopic ellipsometry (SE). The porosity, thickness as well as the refractive index n and the extinction coefficient k of porous GaAs have been estimated. The calculated refractive indices at a fixed wavelength are compared with those obtained theoretically using the Bruggeman effective medium model.

2. EXPERIMENTAL PROCEDURE

Porous GaAs samples were prepared using p-type GaAs (1 0 0) as substrate doped with Zn hole concentration of 10^{18} cm^{-3} by anodization of the substrate in an HF electrolyte under different manufacturing conditions. The samples were then carried out in a Teflon cell with a platinum electrode, under dark conditions. Preparation of samples is made by keeping the HF : Et-OH ratio and the etching time constant at (1:1) and 24 s respectively and varying the current density of anodization. The current anodization is supplied using a Keithley 224 programmable current source. So the current density is to be varied in order to investigate its influence on the porous GaAs characteristics. Before each experiment, the samples are degreased with acetone, propanol and methanol and extensively rinsed with deionized water and then dried by Nitrogen flow. Experimental data on the relationship between the current density and the morphological and optical properties will be discussed in the following sections. The samples data and preparation conditions are summarized in table.1.

Table 1: Growth conditions for porous GaAs

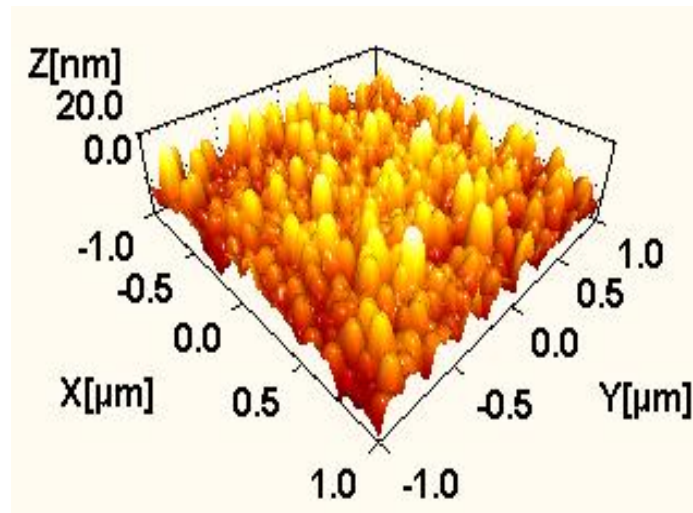
Samples	Current density (mA /Cm ⁻²)	Etching solution	Etching time(s)
Sample A	8	(1 :1)	24
Sample B	24	(1 :1)	24

A detailed view of the top surfaces morphology has been obtained using the atomic force microscopy (AFM), the average size of crystallites formed on porous GaAs samples are estimated using X-Ray diffraction. The optical properties have been investigated by PL measurements. The spectroscopic ellipsometry is used to determine the porosity, thickness, refractive indices and extinction coefficient of porous GaAs layers.

3. RESULTS AND DISCUSSION

3.1 Structural properties of porous GaAs

Porous GaAs has been investigated using atomic force microscopy. AFM measurements were carried out using a Nanoscope 3100 Digital instrument in the tapping mode. The obtained AFM images were processed using the WSxM software ver.5.0 [15]. This software enables to perform a roughness analysis and to estimate the grains dimensions in the samples. Fig.1 depicts the 3D AFM images of p-type porous GaAs formed at applied current densities of 8 mA /Cm^{-2} and 24 mA /Cm^{-2} .



(a)

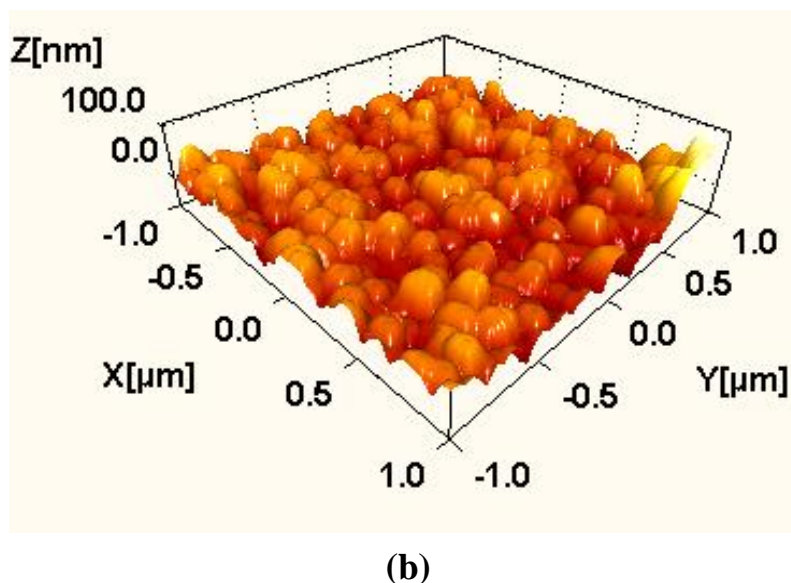


Figure 1: 3D AFM images of porous GaAs: (a) sample A, (b) sample B

The figures indicate the sponge like structure of porous GaAs layers. The top surface of porous GaAs reveals a network of nanometre-sized crystalline GaAs regions surrounded by void space, which represents pores. Distributions of pores and crystallites along the top surfaces have a spheroid shape. The average diameter of crystallites depends on the manufacturing conditions.

When the current etching is raised from 8 to 24mA /Cm⁻², the average pore depth increases from 52 to 154 nm and the porosity decreases from 73 to 57%. The increase rate in the average of pore depth, by raising the etching current density, is appeared to agree well with the proposals of Beale models [17, 18]

The X-Ray curves of porous GaAs structures are acquired by using an X-Ray diffractometry (XRD). Fig.2 shows the XRD spectra of starting GaAs substrate and porous GaAs layers. The XRD of starting GaAs is composed of two intense peaks located at 31,75° and 66,1° (Fig.2.a). They are attributed to the (200) and (400) orientations, respectively. The porous GaAs samples (A and B) show one peak which is associated to the (400) orientation (Fig.2b and Fig.2c) with a broad peak and low intensity. The presence of one peak associated to a particular orientation of pristine GaAs means that the porous layer has the same crystallographic orientation as the starting substrate and simultaneously has a very high crystal line quality. The broadness of (400) diffraction peak is a characteristic of the presence of nanocrystallites formed under anodization. From Fig.2, it can be observed that the rocking curve width of the peak from porous layers is larger than the substrate; this is due to size of the lattice constant. The width of the peak of porous GaAs increases from sample A to sample B, when the current density increases. This is due the manufacturing conditions of undergone of porous GaAs. It is clearly seen that the current density anodization has only a strong effect on the crystalline size formed at the top surface of substrate. Similar behaviours have been observed previously [19- 21] for anodization of GaP in aqueous solutions of sulfur acid. The surface roughness of the porous GaAs thin films is characterized from RMS (root square of the roughness) measurements. The porous GaAs elaborated under lower current density has a low RMS, and this reveals a good surface quality.

However, a relatively large variation of the peak intensities is found for the porous samples, which is related to the slight change of the crystalline quality after etching. The increase in diffraction intensity, resulting from the anodic dissolution process, indicates that the GaAs(100) surface became rough. To explain the increasing trend of the diffraction intensity, two possible reasons can be proposed: (i) the inhomogeneous dissolution of the GaAs (100) surface is expected to occur during electrochemical and chemical etching [22, 23], (ii) the formation of materials such as oxide and As, which absorb the X-ray beam. Similar results are founded by Lingier and Gomes [24].

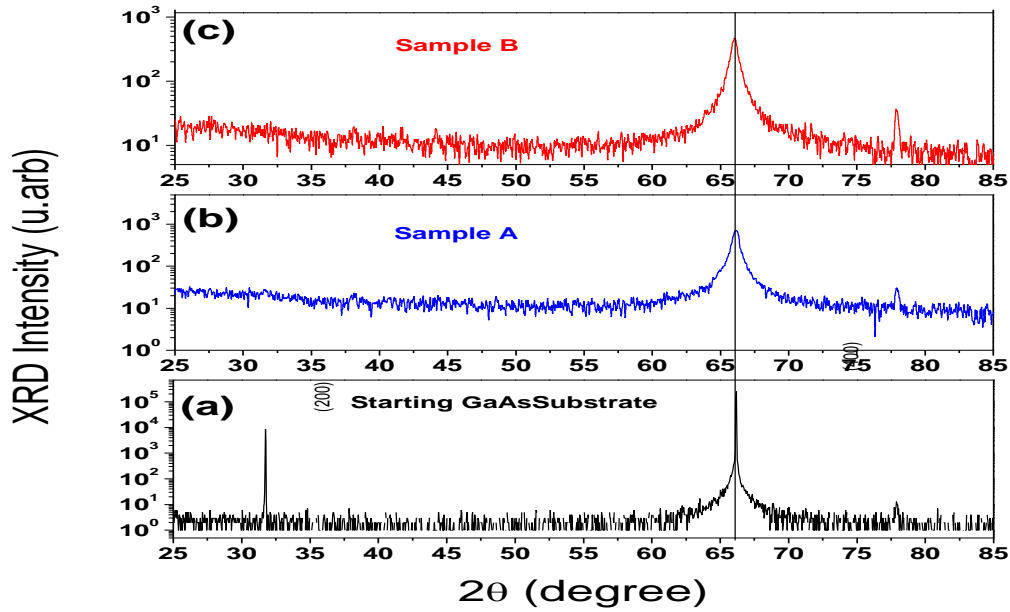


Figure 2: XRD patterns of starting GaAs and porous GaAs layers: (a) substrate, (b) sample A and (c) sample B.

The average crystallite size, corresponding to the average diameter of crystallites was determined using the Debye-Scherrer formula

$$d = \frac{0.9\lambda}{t_{1/2} \cos\theta} \quad (1)$$

where $t_{1/2}$ is the full width at half maximum for the diffraction peak and θ is the diffraction angle. $\theta = 1.54^\circ$ for the $\text{Cu}\alpha$ line. The crystalline size, as deduced from diffraction measurements, shows a decreasing tendency from 32 to 20 nm as the current density increases from 8 to 24 mA /Cm-2. The XRD results are in good agreement with the AFM results obtained during the anodic dissolution process [25]. From the obtained results, we conclude that the pore sizes, porosity and the thicknesses of porous layers are affected by the current density of electrochemical anodization. RMS and porosity parameters are calculated from AFM data and crystalline sizes are estimated from XRD analysis. These different parameters are listed in Table 2.

3.2 Optical properties of porous GaAs

The photoluminescence (PL) spectra of GaAs substrate and p-type porous GaAs formed using different current densities (from 8 mA /Cm-2 to 24 mA /Cm-2) are displayed in Fig.3. It can be seen that, for the GaAs substrate, the PL spectrum shows an infrared peak located at 1.42 eV (871 nm). For the porous GaAs (samples A and B), a visible PL peak is observed at 1.846 eV (677, 5 nm). As the anodization increases, the PL spectrum of porous GaAs reveals two peaks: an infrared peak at 1.42 eV (871 nm) and the visible PL peak at 1.80 eV (688 nm). The infrared PL peak is associated with the near-band edge luminescence of bulk GaAs while the visible PL band is due to quantum confinement-induced transitions in GaAs crystallites formed by electrochemical etching. As is also found, the visible luminescence band is more intense than the infrared PL peak. This difference in intensity is probably attributed to the density of micro- and nanocrystallites. On the other hand, it is interesting to note that the PL intensity of porous GaAs increase as the etching current density increases, accompanied by a blue shift of the corresponding PL spectrum. These features are caused by the increase in the total volume of the nano-crystallites on the surface of porous GaAs.

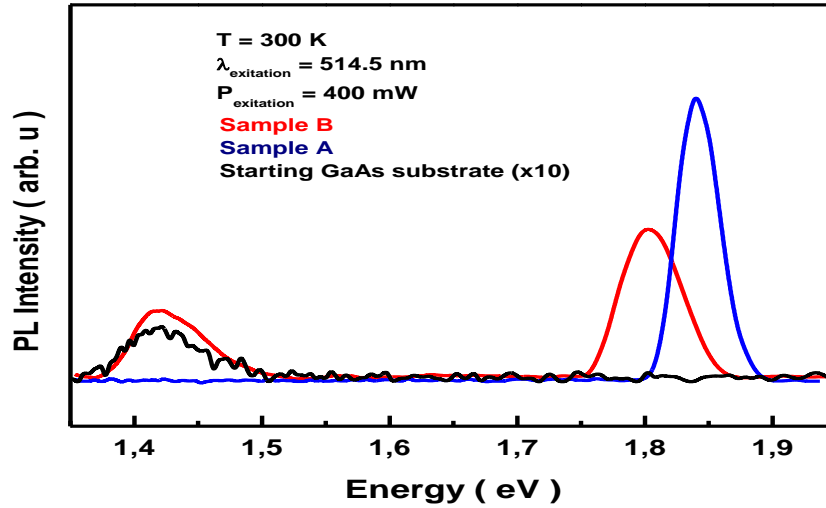


Figure 3: PL spectra of starting GaAs substrate and porous GaAs samples (A and B)

In order to examine the influence of the microstructural characteristics on the optical properties of porous GaAs, spectroscopical ellipsometric measurements were performed and the refractive index and extinction coefficients of the structures studied have been determined. Explanation of the ellipsometric measurements requires the development of an optical model able to describe accurately the surface structures. To extract the refractive index, $n(\lambda)$, and the extinction coefficient $k(\lambda)$ from the ellipsometry data, an inhomogeneous model is considered where both refractive index and extinction coefficient depend on the depth parameter. Generally, porous GaAs materials have an homogenous mixture of air and GaAs. From the optical view point, in the visible and infrared wavelength ranges, porous GaAs can be specified as an effective medium, whose optical properties depend on the relative volumes of GaAs and the pore filling medium, i.e. mainly on the porosity and on the degree of oxidation of the porous GaAs layer [26]. Thus, the optical properties of porous GaAs can be modeled as a mixture of crystalline GaAs and air (“void”) in an effective medium approximation (EMA) [27- 29]. According to this model, porous GaAs is assumed to be an optically isotropic medium with an effective refractive index n_{π} -GaAs. The Bruggeman equation for the two-component system reads as:

$$(1 - p) \frac{n_{\text{GaAs}}^2 - n_{\pi\text{-GaAs}}^2}{n_{\text{GaAs}}^2 + n_{\pi\text{-GaAs}}^2} + p \frac{n_{\text{pore}}^2 - n_{\pi\text{-GaAs}}^2}{n_{\text{pore}}^2 + 2n_{\pi\text{-GaAs}}^2} = 0 \quad (2)$$

where n_{π} -GaAs is the effective refractive index of porous GaAs, n_{GaAs} is the refractive index of crystalline GaAs, n_{pore} is the index refractive of void space ($n = 1$) and p and $(1-p)$ are the volume fractions of pores (void space) and GaAs GaAs respectively in porous layers.

Using this approximation, the effective refractive index of porous GaAs can be calculated according to the relationship:

$$n_{\pi\text{-GaAs}}^{\text{EMA}} = 0.5 \left[3p(1 - n_{\text{GaAs}}^2) + (2n_{\text{GaAs}}^2 - 1) + \left(\left(3p(1 - n_{\text{GaAs}}^2) + (2n_{\text{GaAs}}^2 - 1) \right)^2 + 8n_{\text{GaAs}}^2 \right)^{0.5} \right]^{0.5} \quad (3)$$

Fig. 4(a), 4(b) and 4(c) exhibit the refractive index and the extinction coefficient of starting GaAs and porous GaAs samples as a function of wavelength in visible range (380 -740 nm) and infrared spectral ranges ($\lambda > 740$ nm).

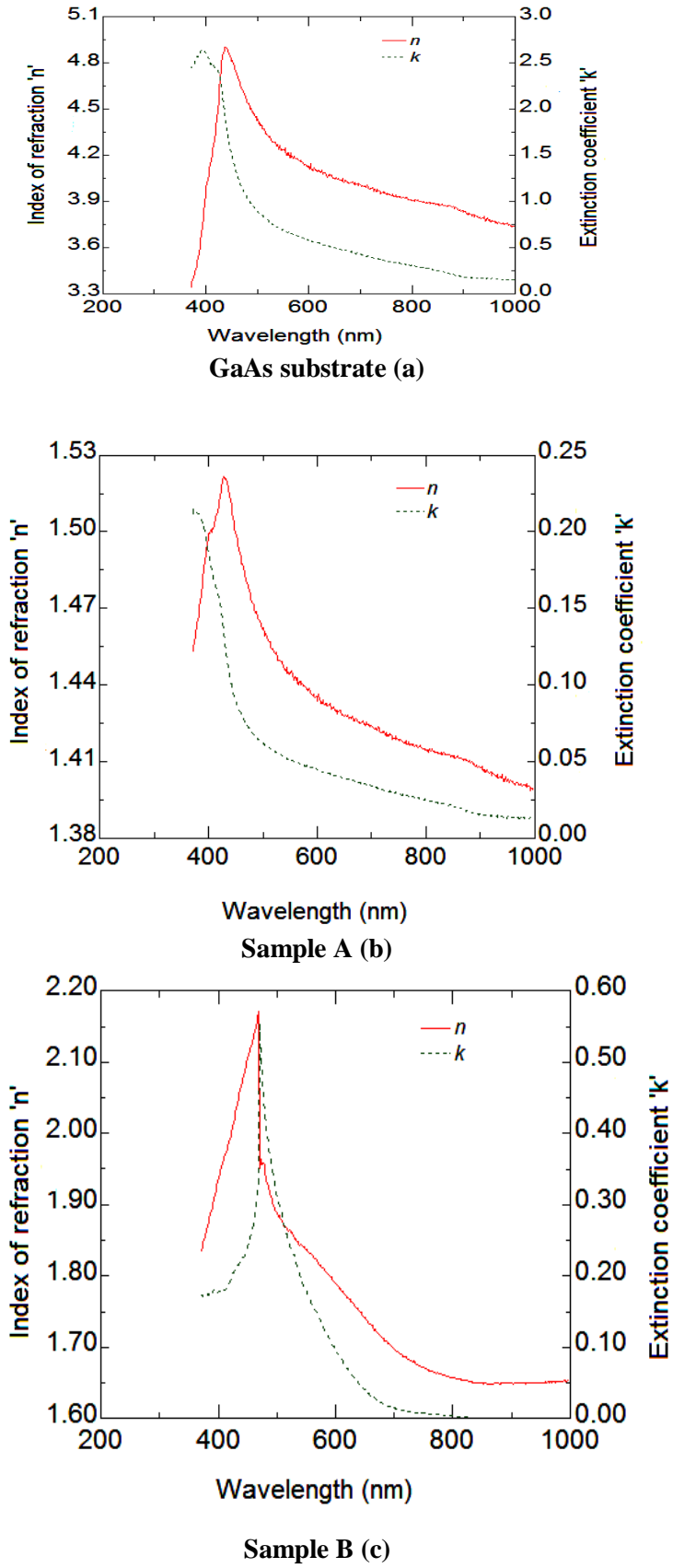


Figure 4: Refractive index and extinction coefficients versus wavelength for : (a) GaAs substrate, (b) porous GaAs(A) and (c) porous GaAs (B)

As seen, the refractive index shows an anomalous dispersion. Indeed, strong index refraction and extinction coefficient peaks are located at around 450 nm. These peaks are probably related to the sizes and morphology of the pores network, which induce a light scattering diffusion effect. The increase of n at high energy side ($\lambda < 450$ nm) indicates that the pores are filled with materials having higher refractive index, which is a oxide layer formed under anodization technique. The decrease of n at the low energy side could be, however, due to the important concentrations of pores, The presence of a native oxide layer at the surface of samples can affect the dielectric function parameters.

Theoretically, the refractive index of porous GaAs has been calculated by using the EMA model. The method is based on calculating the effective refractive index (n_{π} -GaAs) of porous GaAs by using Eq. (3). Optical constant of bulk GaAs at 632nm, is of 4.09 according to that reported in refs [30, 31]. The refractive indices, as calculated for the samples A and B are 1.42 and 1.74, respectively. Obtained results reveal a good agreement between experimental optical data and EMA modeling. As it was demonstrated above, spectroscopic ellipsometry study shows a slight increase in the refractive index at 630 nm correlated to a decrease in the important thickness of oxide layer and the low density of pores. So, the refractive indices are also affected by the density of voids and their occupied volume fraction within porous layers of GaAs. The porosity and the thickness, as estimated from spectroscopic ellipsometry measurements and the refractive index calculations via EMA models of porous GaAs are summarized in the Table.2.

Table 2: Structural parameters calculated from XRD diffraction (d_{XRD} , Porosity, RMS) and spectroscopic ellipsometry measurements (Thickness, porosity, n_{EMA})

Samples	Crystalline size (d_{XRD}) (nm)	Porosity(AFM) %	RMS	Porosity(SE) %	Thickness (nm)	Refractive index(n_{EMA})
Sample A	32	73	5.6	78	52	1.42
Sample B	20	57	20.6	68	154	1.74

4. CONCLUSION

Porous GaAs was prepared by electrochemical anodic etching of p-type GaAs wafers. The structural and optical features of the porous GaAs have been investigated. Distributions of pores and crystallites along the top surfaces of porous GaAs have spheroid shape and the average diameter of crystallites depends on the manufacturing conditions. The obtained values of crystalline sizes of porous GaAs, as deduced from XRD measurements, are in good agreement with AFM results obtained during the anodic dissolution process. The diameter and depth of the column-shaped pores are substantially affected by the etching current density. From PL analysis, the porous GaAs is revealed to exhibit specific features in the visible spectral range. Indeed, the PL intensity of porous GaAs increases and simultaneously the luminescence peak shows a blue shift as the current density increases. It seems that the quantum confinement causes significant changes in the PL of the as-prepared porous GaAs layer. From spectroscopic ellipsometry, the obtained values of the refractive index show an anomalous dispersion and are mainly governed by the sizes and morphology of pores network, leading to a light scattering diffusion. According to the EMA model, the calculated optical effective parameters are in a good agreement with experimental optical data.

REFERENCES

- [1] R.Herino, G. Bomchil, K. Barla, C. Bertrand, and J. L. Ginoux, "Porosity and pore size distributions of porous silicon layers," Journal of the Electrochemical Society, vol. 134, no. 8, pp. 1994–2000, 1987
- [2] L.T. Canham, Appl. Phys. Lett. 57 (1990) 1046
- [3] D.J. Lockwood, Light Emission in Silicon, Academic Press, San Diego, 1997
- [4] A.G. Cullis, L.T. Canham, P.D.J. Calcott, J. Appl. Phys. 82 (1997) 909
- [5] T. Takizawa, S. Arai, M. Nakahara, Jpn. J. Appl. Phys. Part 1, 33 (1994) 2643
- [6] N.G. Ferreira, D. Soltz, F. Decker, L. Cescato, J. Electrochem. Soc. 142 (1995) 1348
- [7] A.I. Belogrokhov, V.A. Karavanskii, A.N. Obraztsov, V.Yu. Timoshenko, JETP Lett. 60 (1994) 275
- [8] A. Meyerink, A.A. Bol, J.J. Kelly, Appl. Phys. Lett. 69 (1996) 2801
- [9] M.I.J. Beale, J.D. Benjamin, M.J. Uren, N.G. Chew, A.G. Cullis, J. Crystal. Growth 73 (1985) 622.]
- [10] R.A. Smith, H. Ahmed, Appl. Phys. Lett. 81 (8) (2002) 1506.
- [11] A.A. Lebedev, Yu.V. Rud, Tech. Phys. Lett. 22 (1996) 483

- [12] P. Schmuki, D. J. Lockwood, H. J. Labbé, and J. W. Fraser, *Appl. Phys. Lett.* 69, 1620, 1996.
- [13] M. Rojas-López, M. A. Vidal, H. Navarro-Contreras, J. M. Gracia-Jiménez, E. Gómez, R. Silva-González, *J. Appl. Phys.* 87 (2000) 1270.
- [14] G. Oskam, A. Natarajan, P.C. Searson, and F.M. Ross, *Appl. Surf. Sci.* 119, 160 (1997)
- [15] P. Schmuki, J. Fraser, C.M. Vitus, M.J. Graham, and H.S. Isaacs. *J. Electrochem. Soc.*, 143(10):3316, 1996.
- [16] A.I. Belogorokhov, S.A. Gavrilov, I.A. Belogorokhov, Structural and optical properties of porous gallium arsenide. *Phys. Status solidi (c)* 2(9), p. 3491-3494 (2005)
- [17] A. Richter, P. Steiner, F. Kozolowski and W. Lang, *IEEE Electron Device Lett.* 31, 1288 (1995)
- [18] M. I. J. Beale, J. D. Benjamin, M. J. Uren, N. G. Chew and A. G. Cullis, *J. Cryst. Growth* 73, 622 (1985).
- [19] L. Santinacci, T. Djenizian, C.R. *Chimie* 11, 964 (2008).]
- [20] B.H. Ern , D. Vanmaekelbergh, J.J. Kelly, *Adv. Mater.* 7, 739 (1995)
- [21] B.H. Ern , D. Vanmaekelbergh, J.J. Kelly, *J. Electrochem. Soc.* 143, 305 (1996)
- [22] W.P. Gomes, H.H. Goossens, in: H. Gedscher, C.W. Tobias (Eds.), *Advances in Electrochemical Science and Engineering*, vol. 3, VCH. New York, 1994, section I
- [23] R. Bhat, S.K. Ghandhi, *J. Electrochem. Soc.* 124 (1977) 1447.
- [24] S. Lingier, W.P. Gomes, *Ber. Bunsenges. Phys. Chem.* 95 (1991), 17
- [25] Yon.J .J, Barla K, Herino.R and Bomchill.G, *J.Appl .Phys.*62, 1042(1987)
- [26] L.T. Canham, *Properties of Porous Silicon*, IEE, INSPEC, London, 1997, pp. 3–43 and 223–246
- [27] L.A.A. Pettersson, L. Hultman, H. Arwin, *Appl. Opt.* 37 (1998) 4130
- [28] U. Rossow, et al., *Thin Solid Films* 255 (1995) 5.
- [29] P. Petrik, et al. *J. Appl. Phys.* 105 (2009) 024908
- [30] H.W.Dinges, *Thin Solid Films*, 50 (1978) L17- L20.
- [31] G.E.Jellison Jr, *Optical Materials*1 (1992), 151,160.